Effects of surface finish and mechanical training on Ni-Ti sheets for elastocaloric cooling

Engelbrecht, Kurt; Tusek, Jaka; Sanna, Simone; Eriksen, Dan; Mishin, Oleg; Bahl, Christian; Pryds, Nini

Published in:
A P L Materials

Link to article, DOI:
10.1063/1.4955131

Publication date:
2016

Document Version
Publisher's PDF, also known as Version of record

AIP | APL Materials

Effects of surface finish and mechanical training on Ni-Ti sheets for elastocaloric cooling

Kurt Engelbrecht, Jaka Tušek, Simone Sanna, Dan Eriksen, Oleg V. Mishin, Christian R. H. Bahl, and Nini Pryds

Citation: APL Mater. **4**, 064110 (2016); doi: 10.1063/1.4955131
View online: http://dx.doi.org/10.1063/1.4955131
View Table of Contents: http://scitation.aip.org/content/aip/journal/aplmater/4/6?ver=pdfcov
Published by the AIP Publishing

Effects of surface finish and mechanical training on Ni-Ti sheets for elastocaloric cooling

Kurt Engelbrecht,[1,a] Jaka Tušek,[1,2] Simone Sanna,[1] Dan Eriksen,[1]
Oleg V. Mishin,[3] Christian R. H. Bahl,[1] and Nini Pryds[1]
[1]*Department of Energy Conversion and Storage, Technical University of Denmark, DK-4000 Roskilde, Denmark*
[2]*Faculty of Mechanical Engineering, University of Ljubljana, Aškerčeva 6, 1000 Ljubljana, Slovenia*
[3]*Department of Wind Energy, Technical University of Denmark, DK-4000 Roskilde, Denmark*

(Received 15 March 2016; accepted 17 June 2016; published online 28 June 2016)

Elastocaloric cooling has emerged as a promising alternative to vapor compression in recent years. Although the technology has the potential to be more efficient than current technologies, there are many technical challenges that must be overcome to realize devices with high performance and acceptable durability. We study the effects of surface finish and training techniques on dog bone shaped polycrystalline samples of NiTi. The fatigue life of several samples with four different surface finishes was measured and it was shown that a smooth surface, especially at the edges, greatly improved fatigue life. The effects of training both on the structure of the materials and the thermal response to an applied strain was studied. The load profile for the first few cycles was shown to change the thermal response to strain, the structure of the material at failure while the final structure of the material was weakly influenced by the surface finish. [http://dx.doi.org/10.1063/1.4955131]

One manifestation of the elastocaloric effect is a temperature change of materials associated with the application or release of a mechanical strain.[1–4] It is generally associated with shape memory alloys and superelastic materials. When the straining and releasing of the material is coupled to interaction with hot and cold reservoirs, a thermodynamic cycle can be built that enables a cooling load to be accepted at temperatures below ambient. Elastocaloric cooling is an alternative cooling technology that has been identified by a US Department of Energy report as the most promising technology to reduce energy consumption for refrigeration and space cooling.[5] Modeling has shown that elastocaloric coolers can operate efficiently when using a regenerative cycle and exhibit much higher specific cooling power than other so-called caloric cooling technologies.[6] However, current elastocaloric devices are relatively simple and have not yet demonstrated adequate temperature spans for use in common space cooling or refrigeration technologies.[7–9]

Compact and efficient elastocaloric coolers in practical use will require high-performance and low hysteresis materials that can withstand millions of mechanical cycles. In recent years, several new elastocaloric materials (eCMs) have been reported[10] in addition to magnetic shape memory alloys[11] and shape memory polymers,[12] which are not considered here. The elastocaloric materials can generally be divided into three groups: Ni-Ti-based alloys,[13–16] Cu-based alloys,[17] and Fe-based alloys.[18] Polycrystalline thin films of Ni-Ti-Cu-Co have been shown to last over 10×10^6 cycles[19] under superelastic conditions, but long fatigue life in bulk elastocaloric samples has not yet been demonstrated. One aspect of eCMs that has not been studied in detail in the literature is how the temperature change in the material is affected by surface roughness and mechanical training. The temperature response and temperature distribution as a function of strain rate and thermal

[a]kuen@dtu.dk

TABLE I. Sample information for each of the six samples tested. Each sample has an active length of 40 mm, a width of 10 mm, and a thickness of 0.2 mm.

Sample	Cutting	Polishing	Training	Cycles to failure
1	water jet	none	none	97
2	EDM fast	none	none	323
3	EDM slow	none	none	1167
4	EDM fast	mech.	none	4569
5	water jet	mech.	at 292 K	1225
6	water jet	mech.	at 318 K	2030

conditions have been reported and shown to be localized according to the transition from austenite to martensite.[14,20–24] In this paper, the temperature distribution of polycrystalline Ni-Ti sheets with an applied strain is studied and methods for homogenizing the temperature response are presented. The effects of surface finish, cutting technique, and mechanical training are all presented and it is shown that mechanical training under isothermal conditions changes the crystal structure of the sample and gives a more even temperature response to strain. Ni-Ti sheets with a thickness of 0.2 mm and mass fraction of $Ni_{0.558}$ $Ti_{0.442}$ were received from Memry GmbH. This material is characterized by an austenitic finish temperature of 280 ± 5 K. An electron backscatter diffraction analysis of these sheets revealed a well-developed $\{111\}\langle uvw\rangle$ texture, which is frequently observed in rolled Ni-Ti.[25] The sheets were cut to dog-bone shaped samples according to ASTM standard E8/E8M with a gauge width of 10 mm such that the strain direction is the same as the rolling direction. Based on microscopy, the unpolished surface appeared to be etched. Three different cutting techniques and two different surface treatments were studied: water jet cutting, a fast high-power electrical discharge machining (EDM) technique, and a slow lower-power EDM technique. The sample preparations are summarized in Table I. Mechanical polishing consists of starting from fine grit sandpaper and moving to wax compounds and a buffing wheel. Polishing was performed in the direction of strain application to avoid small cracks in the direction perpendicular to the strain direction that would lead to premature failure.

Scanning electron microscopy (SEM) images for samples 1–4 are shown in Fig. 1. Samples 5 and 6 were produced with a slightly different cutting technique than the other samples because they were initially water jet cut before polishing. Samples 5 and 6 were also polished separately from the other samples. Therefore, the fatigue life of samples 5 and 6 may not be comparable to sample 4, which was prepared in a different manner. Training consists of performing 300 isothermal cycles at a strain rate of $0.000\,33\ s^{-1}$ to a strain of 0.05, which is similar to stabilization techniques suggested elsewhere.[15,16,26–28] It is important to note that only samples 5 and 6 were trained. Before fatigue testing, each sample was coated with a thin layer of graphite paint that had an emissivity of 0.95 to give a reliable temperature reading with an infrared (IR) camera.

All mechanical tests were performed on a Zwick/Roell EZ030 electro-mechanical testing actuator with an Xforce K load cell that had a 30 kN capacity and uncertainty of 1% and mechanical T-fatigue grips. The strain was measured based on the derivative of the displacement of the crosshead, thereby measuring global or average strain over the sample. Since the sample's width and therefore strain was not constant over the length of the sample, the strains reported here should be considered estimated values based on the equivalent gauge length. Each sample was cycled until failure using the following sequence: the sample was preloaded to 5 MPa, strained at a rate of $0.05\ s^{-1}$ to a final strain of 0.05, held for 2 s, strained at a rate of $0.05\ s^{-1}$ to a stress of 5 MPa, then held for 2 s. The sequence was repeated until the sample failed. All experiments were conducted in air with no forced convection thus the loading and unloading can be considered quasi-adiabatic. The use of a stress constraint during unloading reduced the risk of bending and allowed the sample to deform without going slack when returning to the end of the loading cycle. During testing, all samples experienced some plastic deformation, as is generally observed in elastocaloric Ni-Ti samples.[26] The deformation means that the final length of each sample remained constant, but the starting length increased with cycle number, and thus the change in length decreased. Although the

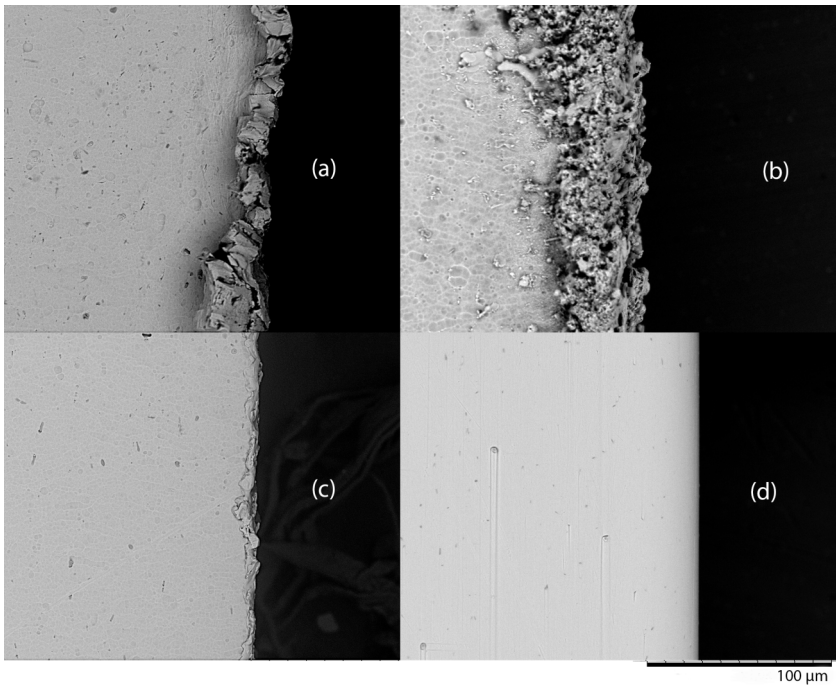

FIG. 1. SEM images of the edges of the four surface finishes investigated in this work (a) sample 1, (b) sample 2, (c) sample 3, (d) sample 4.

force constraint during unloading was made to prevent the sample from buckling, the response time of the mechanical tester was not fast enough to avoid buckling in the samples during unloading. All samples experienced bending during unloading, which likely influenced the fatigue life. The number of loading and unloading cycles that each sample underwent before failure is given in Table I. Sample 5 and 6 had a fatigue life longer than sample 3 but shorter than sample 4. Sample 6 had a longer fatigue life than sample 5, suggesting that training at higher temperature increases fatigue life. The fact that samples 1–3 withstood only very small numbers of cycles to failure clearly demonstrates that surface finish has a huge influence on the fatigue life of the samples.

The thermal response of each sample during fatigue testing was measured with a FLIR SC5200 IR camera for the first several cycles at a strain rate of 0.05 s^{-1}. In order to capture fast temperature changes, the thermal images were acquired with a frame-rate of up to 150 Hz. A still frame of each of the six samples during loading and unloading of the first fatigue cycle is shown in Fig. 2 (Multimedia view), captured as the top grip on the mechanical tester moved up or down during the loading cycle. The precise strain for which the images were captured is not known because each image was extracted from the video at some intermediate strain where the transformation has started but has not yet reached the final strain, where the temperature of the sample will be much more homogeneous. The estimated strain for each image is 0.03 during loading. There are some artifacts visible in the images, most notably on the mechanical grips of the tester. The grips could not be painted with graphite and the bare metal caused reflections. This adds uncertainty to the measured temperatures, but these results are used for visualization and not for property measurement. Because the IR response was measured on the samples during the first cycle, the adiabatic temperature change was the highest for the cycles recorded. Generally, the elastocaloric effect was observed to be more homogeneous during unloading than loading.

As can be seen in the figure, the untrained samples, 1-4, have a similar thermal response to one another. All four samples show relatively thin Lüders bands[29] rising from both the left and the right. Some bands intersect, while others span the width of the sample or terminate when they intersect another band. The results for the untrained samples are similar to those reported in Ref. 23. As

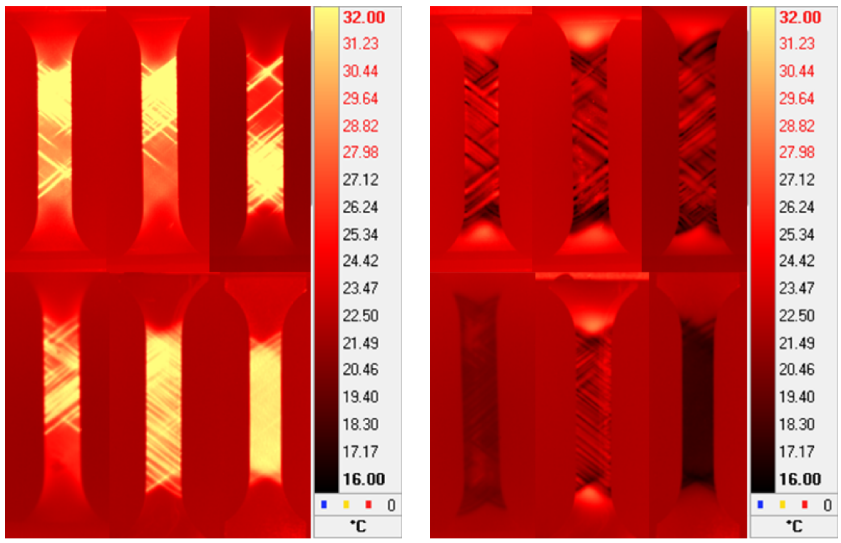

(a) (b)

FIG. 2. IR images of each sample listed in Table I during the loading (a) and during unloading (b). Top row left to right: sample 1, sample 2, sample 3. Bottom row, left to right: sample 4, sample 5, sample 6. The width of the sample is 10 mm for each image. (Multimedia view) [URL: http://dx.doi.org/10.1063/1.4955131.1]

discussed in Ref. 23, the narrow bands are caused by stiffening of the material at the phase boundaries due to self-heating during strain. If the strain were applied under isothermal conditions, there would have been fewer bands growing in width during loading. In order to measure the angle of the bands, the edge of several bands were detected from the IR image using edge detection algorithms in MATLAB, then polynomials were fit to the edges and the intersection angle was then calculated. Band angles were only measured for the untrained samples because the distance between bands coupled with the IR camera resolution did not allow for edge detection of the Lüders bands in the trained samples. The angle of intersection was not found to be a function of the edge roughness and the bands were between 50.2° and 54.9° to the strain axis. These values are between the 48° angle reported by Ref. 20 for relatively high strain rates and the 55° angle reported by Refs. 30 and 31 for isothermal conditions. The Lüders bands for the two trained samples (5 and 6) are much more evenly distributed throughout the sample and seem to be "woven" together by bands in a criss-cross pattern across the sample. While untrained samples tend to exhibit larger temperature changes that start in one area of the sample and then move across the sample until it is fully strained and at a uniform temperature, the trained samples show a much more homogeneous IR response to strain. For sample 6, which was trained at the highest temperature and therefore the highest stress, the bands are so tightly woven that the entire specimen exhibits a nearly equal IR response on the macro-scale. The adiabatic temperature change with strain of sample 6 was smaller than those of the other samples due to training effects, as also observed by Refs. 15 and 16. Videos of strain applications for samples 4–6 are available in Fig. 2 (Multimedia view). Samples 5 and 6 exhibit a more desirable IR response for elastocaloric cooling applications, and similar results were achieved by training Ni-Ti wires[15] and NiTiCuV ribbons.[16]

The nature of the IR response to mechanical training was studied by attaching a macro-lens focused on an area of approximately 3 mm × 2 mm to the IR camera and recording the response to applying and releasing a strain. A still image of the video is shown in Fig. 3. In the IR image, bands with large temperature changes exist on a small scale, and they are separated by regions of untransformed material. The active regions are interlinked by nearly orthogonal bands of the active material. The IR response suggests that the width of the Lüders bands is slightly less than 1 mm. The bands seem to be evenly spaced and structured and the bands intersect each other at multiple points.

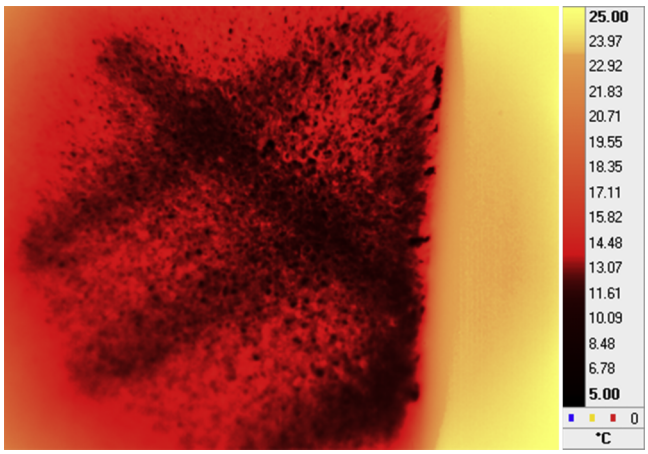

FIG. 3. A closeup IR image of sample 5 during unloading at a strain rate of 0.05 s^{-1}. The area of the image is approximately 3×2 mm^2.

After failure, each sample was analyzed using X-ray diffraction (XRD) to see if there is a change in the crystal structure during operation. The phase characterization of the samples was carried out using a diffractometer (Bruker AXS D8 Discover) in a Bragg–Brentano θ–2θ configuration, with a Cu Kα source (1.5418 Å), over a θ–2θ angular range of 20°–110°. A virgin sample that had not been polished or mechanically cycled was used as a reference. There was no clear evidence that martensite was present in samples 1–4. However, for samples 5 and 6, shown in Fig. 4, the typical B19′ phase with (002) and (11-1) diffraction peaks combined with a sizable decrease of the (110) B2 austenite peak can be distinguished. This suggests that training builds up residual martensite in these two samples, which may explain the plastic deformation that the samples experienced during testing.[32] Calorimetry analysis of trained samples has also been reported[16] and training was shown to also modify the specific heat of elastocaloric materials. The IR response of these samples in Figs. 2 (Multimedia view) and 3 suggests that the martensite in the trained samples 5 and 6 is evenly distributed throughout these samples. Although no clear evidence of martensite was obtained based on XRD measurements for samples 1–4, the plastic deformation observed during mechanical testing suggests that some residual martensite was accumulated also in these samples.

In conclusion it was shown the mechanical training of an eCM can give a much more homogeneous temperature response to an applied strain compared to an untrained sample. XRD analysis suggests that the improved response may be due to a buildup of martensite throughout the trained samples 5 and 6. IR imaging of the trained samples shows that there is a banded structure in the

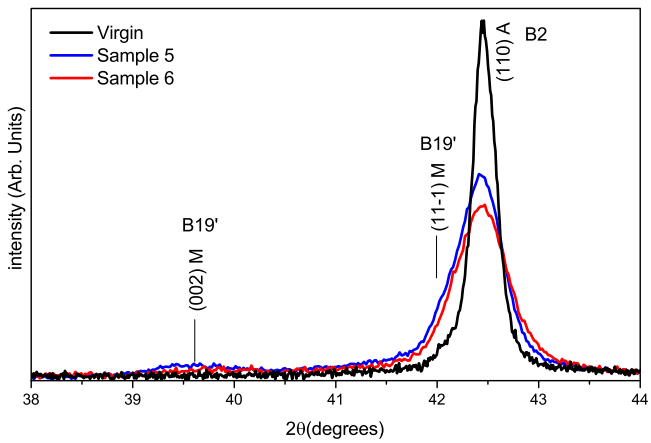

FIG. 4. XRD results for samples 5 and 6 after failure compared to a virgin sample.

regions that are active. Mechanical training of samples is therefore recommended when using eCMs in cooling devices. Results of fatigue tests of eCMs under conditions expected in cooling devices indicate that the fatigue life of superelastic materials is greatly affected by surface finish, which is in accordance with fatigue studies for other materials.[33,34]

Jaka Tušek would like to acknowledge the support of DTU's international H. C. Ørsted postdoc and the Slovenian Research Agency (project No. Z2-7219) for supporting this work.

[1] S. Fähler, U. K. Rößler, O. Kastner, J. Eckert, G. Eggeler, H. Emmerich, P. Entel, S. Müller, E. Quandt, and K. Albe, Adv. Energy Mater. **14**, 10 (2012).
[2] X. Moya, S. Kar-Narayan, and N. D. Mathur, Nat. Mater. **13**, 439 (2014).
[3] A. Kitanovski, U. Plaznik, U. Tomc, and A. Poredoš, Int. J. Refrig. **57**, 288 (2015).
[4] S. Qian, D. Nasuta, A. Rhoads, Y. Wang, Y. Geng, Y. Hwang, R. Radermacher, and I. Takeuchi, Int. J. Refrig. **62**, 177 (2016).
[5] W. Goetzler, R. Zogg, J. Young, and C. Johnson, "Energy savings potential and RD&D opportunities for non-vapor-compression HVAC technologies," Technical Report DOE/EE-1021, Navigant Consulting, Inc., prepared for U.S. Department of Energy, 2014.
[6] J. Tušek, K. Engelbrecht, R. Millán-Solsona, L. Mañosa, E. Vives, L. P. Mikkelsen, and N. Pryds, Adv. Energy Mater. **5**, 1500361 (2015).
[7] H. Ossmer, S. Miyazaki, and M. Kohl, in *18th International Conference on Solid-State Sensors, Actuators & Microsystems (TRANSDUCERS)* (IEEE, 2015), pp. 726–729.
[8] M. Schmidt, A. Schütze, and S. Seelecke, Int. J. Refrig. **54**, 88 (2015).
[9] S. Qian, Y. Wu, J. Ling, J. Muehlbauer, Y. Hwang, I. Takeuchi, and R. Radermacher, in International Congress of Refrigeration 2015, Yokohama, Japan, 16–22 August 2015.
[10] Y. Xu, B. Lu, W. Sun, A. Yan, and J. Liu, Appl. Phys. Lett. **106**, 201903 (2015).
[11] W. Sun, J. Liu, B. Lu, Y. Li, and A. Yan, Scr. Mater. **114**, 1 (2016).
[12] Z. Xie, G. Sebald, and D. Guyomar, Appl. Phys. Lett. **107**, 081905 (2015).
[13] J. Cui, Y. Wu, J. Muehlbauer, Y. Hwang, R. Radermacher, S. Fackle, M. Wuttig, and I. Takeuchi, Appl. Phys. Lett. **101**, 073904 (2012).
[14] H. Ossmer, F. Lambrecht, M. Gültig, C. Chluba, E. Quandt, and M. Kohl, Acta Mater. **81**, 9 (2014).
[15] J. Tušek, K. Engelbrecht, L. P. Mikkelsen, and N. Pryds, J. Appl. Phys. **117**, 124901 (2015).
[16] M. Schmidt, J. Ullrich, A. Wieczorek, J. Frenzel, A. Schütze, G. Eggeler, and S. Seelecke, Shape Mem. Superelasticity **1**, 132 (2015).
[17] L. Manosa, S. Jarque-Farnos, E. Vives, and A. Planes, Appl. Phys. Lett. **103**, 211904 (2013).
[18] F. Xiao, T. Fukuda, T. Kakeshita, and X. Jin, Acta Mater. **87**, 8 (2015).
[19] C. Chluba, W. Ge, R. L. de Miranda, J. Strobel, L. Kienle, E. Quandt, and M. Wuttig, Science **348**, 1004 (2015).
[20] E. Pieczyska, S. Gadaj, W. Nowacki, and H. Tobushi, Exp. Mech. **46**, 531 (2006).
[21] B.-C. Chang, J. A. Shaw, and M. A. Iadicola, Continuum Mech. Thermodyn. **18**, 83 (2006).
[22] J. A. Shaw and S. Kyriakides, Acta Mater. **45**, 683 (1997).
[23] H. Ossmer, C. Chluba, M. Gueltig, E. Quandt, and M. Kohl, Shape Mem. Superelasticity **1**, 142 (2015).
[24] E. Pieczyska, J. Mod. Opt. **57**, 1700 (2010).
[25] E. Hornbogen, G. Brückner, and G. Gottstein, Z. Metallkd. **93**, 3 (2002).
[26] S. Miyazaki, T. Imai, Y. Igo, and K. Otsuka, Metall. Trans. A **17**, 115 (1986).
[27] H. Tobushi, Y. Shimeno, T. Hachisuka, and K. Tanaka, Mech. Mater. **30**, 141 (1998).
[28] J. Olbricht, A. Yawny, A. Condo, F. Lovey, and G. Eggeler, Mater. Sci. Eng.: A **481-482**, 142 (2008).
[29] P. Šittner, Y. Liu, and V. Novak, J. Mech. Phys. Solids **53**, 1719 (2005).
[30] J. A. Shaw and S. Kyriakides, Int. J. Plast. **13**, 837 (1998).
[31] J. A. Shaw, Int. J. Plast. **16**, 541 (2000).
[32] P. Sedmák, P. Šittner, J. Pilch, and C. Curfs, Acta Mater. **94**, 257 (2015).
[33] C. Wiesner, H. Kiinzi, and B. Ilschner, Mater. Sci. Eng.: A **145**, 151 (1991).
[34] P. S. Maiya, Scr. Metall. **9**, 1277 (1975).